Heteroatom Chemistry
Volume 16, Number 5, 2005

Synthesis and Structure of the Scandium-Rich Indides $Sc_5Ni_2In_4$ and $Sc_5Rh_2In_4$

Mar'yana Lukachuk, Birgit Heying, Ute Ch. Rodewald, and Rainer Pöttgen

Institut für Anorganische und Analytische Chemie and NRW Graduate School of Chemistry, Westfälische Wilhelms-Universität Münster, Corrensstraße 36, 48149 Münster, Germany

Received 28 October 2005

ABSTRACT: *The ternary indides $Sc_5Ni_2In_4$ and $Sc_5Rh_2In_4$ were synthesized by arc-melting of the elements and subsequent annealing. A structural investigation by X-ray powder and single crystal diffraction revealed: $Lu_5Ni_2In_4$ type, Pbam, a = 1716.3(2), b = 755.1(1), c = 335.22(5) pm, wR2 = 0.0721, 844 F^2 values for $Sc_5Ni_2In_4$, and a = 1754.3(3), b = 765.0(1), c = 332.97(6) pm, wR2 = 0.0363, 1107 F^2 values for $Sc_5Rh_2In_4$ with 36 variables per refinement. Both structures can be described as intergrowths of distorted AlB_2- and CsCl-related slabs, where the transition metal (T) atoms have a trigonal prismatic and the indium atoms a distorted square prismatic coordination. The shortest interatomic distances occur for Sc—T and T—In. The crystal chemistry and chemical bonding in these intermetallics are briefly discussed.* © 2005 Wiley Periodicals, Inc. Heteroatom Chem 16:364–368, 2005; Published online in Wiley InterScience (www.interscience.wiley.com). DOI 10.1002/hc.20106

INTRODUCTION

Many structures of complex intermetallic compounds in the ternary systems *R*—*T*—*X* (*R* = Ti, Zr, Hf, rare earth or actinoid metal; *T* = late transition metal; *X* = element of the 3rd, 4th, or 5th main group) can be described as intergrowths of slightly distorted slabs that are related to simple binary or ternary structure types such as AlB_2, Cu_3Au, $CaCu_5$, CsCl, $BaAl_4$, NaCl, and others [1–6].

The various intergrowths for the rare earth-transitions metal-indides have recently been reviewed [7]. Several of these indides crystallize with distorted CsCl- and AlB_2- related slabs in different tessellation. Prominent examples are indides with the tetragonal Mo_2FeB_2 [8, 9, and reference. therein], the orthorhombic Mn_2AlB_2 [10], or the orthorhombic $Lu_5Ni_2In_4$- type structure [11]. More than 100 indides crystallize with these three structure types. With the rare earth elements, the indides $RE_5Ni_2In_4$ (*RE* = Ho, Er, Tm, Lu) have been reported [11]. The structure type was determined for $Lu_5Ni_2In_4$, space group *Pbam*, and *Z* = 2.

Due to the lanthanoid contraction, the metallic and the covalent radii of hafnium and zirconium are almost identical [12] although hafnium has about twice the atomic mass. Consequently, zirconium and hafnium have very similar chemical properties and in the field of intermetallics they often form isotypic compounds. During our recent phase analytical investigations in the (Zr, Hf)—*T*—In systems, we obtained the indides $Zr_5Rh_2In_4$ and $Hf_5Rh_2In_4$ [13] which are isotypic with the $RE_5Ni_2In_4$ compounds. $Zr_5Ir_2In_4$ [14] also crystallizes with a pronounced $Lu_5Ni_2In_4$-type subcell; however, weak superstructure reflections require doubling of the subcell *c*-axis. The difference in size between rhodium and iridium

Dedicated to Professor Dr. Alfred Schmidpeter on the occasion of his 75th birthday.

Correspondence to: Rainer Pöttgen; e-mail: pottgen@uni-muenster.de.

Contract grant sponsor: Deutsche Forschungsgemeinschaft.

is most likely responsible for the small structural distortions.

The size of zirconium and hafnium is similar to that of scandium [12], the smallest of the rare earth metals. We have now investigated such scandium compounds and found the new $Lu_5Ni_2In_4$ type indides $Sc_5Ni_2In_4$ and $Sc_5Rh_2In_4$. The synthesis and crystal chemistry of these intermetallics are reported herein.

RESULTS AND DISCUSSION

The structures of $Sc_5Ni_2In_4$ and $Sc_5Rh_2In_4$ have been refined on the basis of single crystal X-ray data. They crystallize with the orthorhombic $Lu_5Ni_2In_4$ type. As an example, we present a projection of the $Sc_5Rh_2In_4$ structure onto the *xy* plane in Fig. 1. Since the structure refinement revealed slightly better values for $Sc_5Rh_2In_4$, in the following discussion we focus on the rhodium compound. From a purely geometrical point of view, the structure can be considered as an intergrowth of distorted CsCl- and AlB_2- related slabs. All indium atoms have a strongly distorted square prismatic coordination, while the smaller rhodium atoms are located in distorted trigonal prisms.

The shortest distances in the $Sc_5Rh_2In_4$ structure occur for Sc—Rh. The latter range from 263 to 279 pm, close to the sum of the covalent radii of 269 pm [12]. Similar trigonal [$RhSc_6$] prisms occur in the indide $Sc_3Rh_{1.594}In_4$ with a new ZrNiAl superstructure [15]. Here, the Sc—Rh distances are 272 and 273 pm. All of these Sc—Rh distances are comparable to those in CsCl-type ScRh (278 pm) [16] and Cu_3Au-type $ScRh_3$ (276 pm) [17]. We can thus assume strong Sc—Rh bonding in $Sc_5Rh_2In_4$.

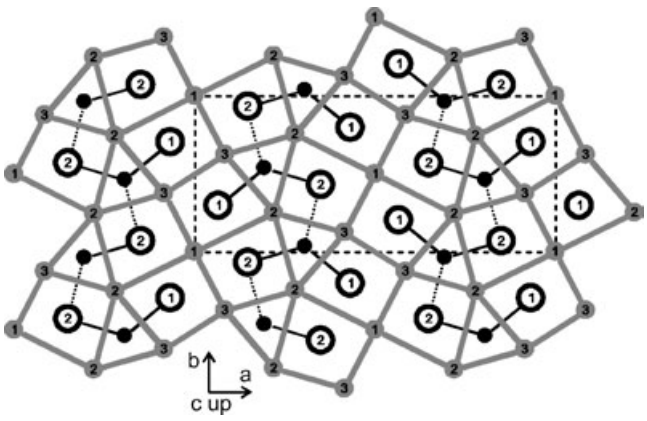

FIGURE 1 Projection of the $Sc_5Rh_2In_4$ structure onto the *xy* plane. All atoms lie on mirror planes at $z = 1/2$ (thin lines) and $z = 1$ (thick lines). Scandium, rhodium, and indium atoms are drawn as medium gray, filled, and open circles, respectively. Atom designations are indicated. The distorted trigonal prismatic rhodium coordination (AlB_2 slab) and the distorted square prismatic indium coordination (CsCl slab) are emphasized. For clarity, only Rh–In bonds are drawn in the [Rh_2In_4] network at $z = 1/2$.

The rhodium and indium atoms at $z = 1/2$ build up two-dimensional [Rh_2In_4] networks as emphasized in Fig. 1. Each rhodium atom has three indium neighbors in an almost trigonal-planar coordination. Two indium neighbors are at Rh—In distances of 285 and 289 pm, while the third indium atom is at 311 pm. The shorter Rh—In distances are only slightly longer than the sum of the covalent radii of 275 pm. The third contact can only be considered as weak as indicated by dotted lines in the figure. Within the network, each indium atom has three close indium neighbors at In—In distances varying from 315 to 333 pm, similar to elemental, tetragonal body-centered indium [18], where each indium atom has four nearest indium neighbors at 325 pm and eight further neighbors at 338 pm. The two-dimensional [Rh_2In_4] networks are thus governed by strong Rh—In and In—In bonding as well. While the Rh—In bonding exclusively occurs within the [Rh_2In_4] layers, the In—In distances at 333 pm (the unit cell *c* axis) condense the layers in the third direction.

Finally we need to comment on the Sc—Sc contacts in this metal-rich indide. Each of the three crystallographically different scandium atoms has between two and four scandium neighbors at relatively short Sc—Sc distances between 323 and 333 pm. The latter corresponds to the unit cell *c* axis. Additionally, a variety of longer Sc—Sc distances between 353 and 396 pm occurs. The shorter Sc—Sc distances are similar to the average Sc—Sc distance of 328 pm in *hcp* scandium [18]. Thus we observe significant Sc—Sc bonding within the scandium layers at $z = 0$ and also between these layers.

For different drawings of the structure and for a more detailed discussion of the crystal chemistry and chemical bonding of the $Lu_5Ni_2In_4$-type intermetallics, we refer to previous manuscripts [11,13,14].

EXPERIMENTAL

Synthesis

Starting materials for the preparation of $Sc_5Ni_2In_4$ and $Sc_5Rh_2In_4$ were scandium ingots (Kelpin), nickel wire (Ø 0.38 mm, Johnson-Matthey), rhodium powder (Degussa, ca. 200 mesh), and indium teardrops (Johnson-Matthey), all with stated purities better than 99.9%). In a first step, pieces of the scandium

ingot were arc melted [19] to small buttons under an argon atmosphere of ca. 600 mbar. The argon was purified before over molecular sieves, silica gel, and titanium sponge (900 K). This premelting procedure strongly reduces shattering during the subsequent reactions. The scandium button, pieces of the nickel wire (a cold-pressed pellet of rhodium), and pieces of the indium tear drops were weighed in the ideal 5:2:4 atomic ratios and arc melted. The resulting buttons were remelted three times in order to ensure homogeneity. The total weight losses after the arc-melting procedures were always smaller than 0.5%.

$Sc_5Ni_2In_4$ and $Sc_5Rh_2In_4$ were obtained only in polycrystalline form by arc melting. For crystal growth, pieces of the arc-melted samples were sealed in small evacuated tantalum tubes [19]. The latter have been enclosed in evacuated silica ampoules for oxidation protection and first rapidly heated at 1320 K for 7 h, cooled at a rate of 3 K/h to 1020 K, then at a rate of 4 K/h to 770 K, and finally quenched by switching off the furnace. Both annealing procedures resulted in loose agglomerates of crystals nicely separated from the polycrystalline material. The samples could quantitatively be separated from the tantalum tubes. No reactions with the crucible material were observed. $Sc_5Ni_2In_4$ and $Sc_5Rh_2In_4$ are stable in moist air over months. Fine-grained powders are dark gray; single crystals exhibit metallic luster.

EDX Analyses

The single crystals investigated on the diffractometer were analyzed with a Leica 420 I scanning electron microscope using Sc, Ni, Rh, and InAs as standards. No metallic impurity elements were detected. Analyses of the single crystals revealed the compositions 45 ± 2 at.% Sc : 16 ± 2 at.% Ni : 39 ± 2 at.% In, and 45 ± 2 at.% Sc : 18 ± 2 at.% Rh : 37 ± 2 at.% In, close to the ideal composition of 45.5 : 18.2 : 36.3. The relatively high standard deviations account for the different measurements and for the irregular surface of the crystals.

X-ray Investigations

Both samples were characterized through Guinier powder patterns after the arc-melting procedure and after the annealing program. The Guinier camera was equipped with an image plate system (Fujifilm BAS-1800). Cu Kα_1 radiation was used and α-quartz ($a = 491.30$ pm, $c = 540.46$ pm) was taken as an internal standard. The lattice parameters (Table 1) were obtained from least-squares fits of the powder data. The correct indexing of the patterns was ensured through intensity calculations [20] taking the atomic positions from the structure refinements. The lattice parameters determined from the powders and the single crystals agreed well.

The lath-shaped silvery single crystals of $Sc_5Ni_2In_4$ and $Sc_5Rh_2In_4$ were strongly agglomerated. As an example we present such an agglomerate of $Sc_5Ni_2In_4$ in Fig. 2. They were carefully separated by mechanical fragmentation and mounted on quartz fibers. They were examined by Laue photographs on a Buerger precession camera (Mo radiation) equipped with an image plate system (Fujifilm BAS-1800) in order to establish suitability for intensity data collection. Single crystal intensity data were collected at room temperature by use of a Stoe IPDS-II diffractometer (oscillation mode) with graphite monochromatized Mo Kα radiation (71.073 pm). Numerical absorption corrections were applied to the data. All relevant crystallographic data and experimental details for both data collections are listed in Table 2.

Structure Refinements

The isotypism of $Sc_5Ni_2In_4$ and $Sc_5Rh_2In_4$ with $Zr_5Rh_2In_4$ [13] was already evident from the X-ray powder data. The systematic extinctions were compatible with the centrosymmetric space group *Pbam*, in agreement with the previous investigations [11,13]. During the integration procedure, the data set was carefully analyzed with respect to superstructure reflections. There was no hint for doubling of the subcell c axis as in $Zr_5Ir_2In_4$ [14]. The atomic parameters of $Zr_5Rh_2In_4$ were used as starting values, and both structures were refined using SHELXL-97 (full-matrix least-squares on F_o^2) [21] with anisotropic atomic displacement parameters for all atoms. In a saeparate series of least-squares cycles, we refined the occupancy parameters to check for

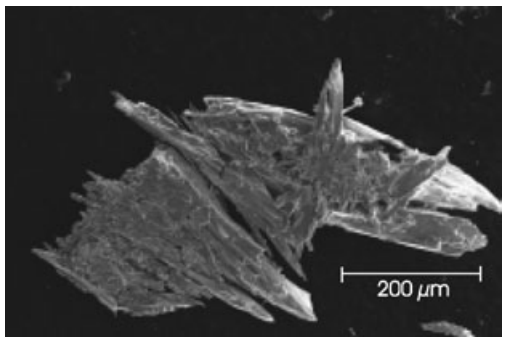

FIGURE 2 Scanning electron micrograph of agglomerated $Sc_5Ni_2In_4$ crystals.

TABLE 1 Lattice Parameters of Orthorhombic Indides with $Lu_5Ni_2In_4$ Type Structure, Space Group *Pbam*. For $Zr_5Ir_2In_4$ only the Subcell Data Are Listed [14]

Compound	*a (pm)*	*b (pm)*	*c (pm)*	*V (nm^3)*	*Ref.*
$Ho_5Ni_2In_4$	1776.8(5)	788.8(3)	356.8(2)	0.5001	[11]
$Er_5Ni_2In_4$	1772.2(8)	786.6(4)	355.8(3)	0.4960	[11]
$Tm_5Ni_2In_4$	1765.3(6)	784.3(3)	354.2(3)	0.4904	[11]
$Lu_5Ni_2In_4$	1756.8(5)	779.8(2)	352.2(1)	0.4825	[11]
$Sc_5Ni_2In_4$	1716.3(2)	755.1(1)	335.22(5)	0.4345	This work
$Sc_5Rh_2In_4$	1754.3(3)	765.0(1)	332.97(6)	0.4469	This work
$Zr_5Rh_2In_4$	1739.8(2)	758.3(1)	337.42(5)	0.4452	[13]
$Hf_5Rh_2In_4$	1732.1(3)	757.5(2)	333.36(7)	0.4374	[13]
$Zr_5Ir_2In_4$	1739.5(6)	766.3(2)	338.9(2)	0.4518	[14]

TABLE 2 Crystal Data and Structure Refinement for $Sc_5Ni_2In_4$ and $Sc_5Rh_2In_4$ (Space Group *Pbam*, Z = 2, oP22)

Empirical formula	$Sc_5Ni_2In_4$	$Sc_5Rh_2In_4$
Molar mass	801.50 g/mol	889.90 g/mol
Unit cell dimensions	Table 1	Table 1
Calculated density	6.13 g/cm^3	6.61 g/cm^3
Crystal size	40 × 40 × 140 μm^3	10 × 20 × 120 μm^3
Transm. ratio (max/min)	2.59	1.82
Absorption coefficient	18.2 mm^{-1}	17.2 mm^{-1}
F(000)	714	782
Detector distance	80 mm	60 mm
Exposure time	14 min	20 min
ω range; increment	0–180°, 1.0°	0–180°, 1.0°
Integr. parameters A, B, EMS	14.5; 4.5; 0.012	14.5; 4.5; 0.014
θ range	2° to 32°	3° to 35°
Range in hkl	± 25, ± 10, ± 4	± 28, ± 12, ± 5
Total no. reflections	4965	6324
Independent reflections	844 (R_{int} = 0.0417)	1107 (R_{int} = 0.0273)
Reflections with $I>2\sigma(I)$	800 (R_{sigma} = 0.0211)	1017 (R_{sigma} = 0.0149)
Data/parameters	844 / 36	1107 / 36
Goodness-of-fit on F^2	1.141	1.148
Final R indices [$I>2\sigma(I)$]	R_1 = 0.0281 wR_2 = 0.0711	R_1 = 0.0186 wR_2 = 0.0352
R indices (all data)	R_1 = 0.0299 wR_2 = 0.0721	R_1 = 0.0230 wR_2 = 0.0363
Extinction coefficient	0.006(1)	0.0028(4)
Largest diff. peak and hole	1.13 and −1.11 e/Å^3	1.05 and –1.18 e/Å^3

TABLE 3 Atomic Coordinates and Isotropic Displacement Parameters (pm^2) for $Sc_5Ni_2In_4$ and $Sc_5Rh_2In_4$

Atom	*Wyckoff Position*	*x*	*y*	*z*	U_{eq}
		$Sc_5Ni_2In_4$			
Sc1	2*a*	0	0	0	118(3)
Sc2	4*g*	0.22052(5)	0.25175(14)	0	124(2)
Sc3	4*g*	0.41445(6)	0.12359(13)	0	117(2)
Ni	4*h*	0.30496(4)	0.03758(10)	1/2	131(2)
In1	4*h*	0.56792(2)	0.20199(5)	1/2	122(1)
In2	4*h*	0.84816(2)	0.07229(5)	1/2	123(1)
		$Sc_5Rh_2In_4$			
Sc1	2*a*	0	0	0	87(1)
Sc2	4*g*	0.22062(4)	0.25443(9)	0	99(1)
Sc3	4*g*	0.41546(4)	0.12507(8)	0	88(1)
Rh	4*h*	0.30569(1)	0.03729(3)	1/2	88(1)
In1	4*h*	0.56739(1)	0.20326(3)	1/2	92(1)
In2	4*h*	0.85026(1)	0.06934(3)	1/2	96(1)

U_{eq} is defined as one third of the trace of the orthogonalized U_{ij} tensor.

deviations from the ideal composition, especially since rhodium and indium differ only by four electrons. Since all sites were fully occupied within two standard deviations, the ideal occupancies were assumed again in the final cycles. Final difference Fourier syntheses revealed no significant residual peaks (Table 2). The positional parameters and interatomic distances are listed in Tables 3 and 4. Further details on the structure refinements may be obtained from: Fachinformationszentrum Karlsruhe, D–76344 Eggenstein-Leopoldshafen (Germany), by quoting the Registry nos. CSD–414505 ($Sc_5Ni_2In_4$) and CSD–414506 ($Sc_5Rh_2In_4$).

TABLE 4 Interatomic Distances (pm), Calculated with the Lattice Parameters Taken from X-ray Powder Data of $Sc_5Ni_2In_4$ and $Sc_5Rh_2In_4$

$Sc_5Ni_2In_4$				$Sc_5Rh_2In_4$			
Sc1:	4	In1	303.8	Sc1:	4	In1	305.3
	4	In2	314.6		4	In2	315.5
	2	Sc3	319.9		2	Sc3	322.9
	2	Sc1	335.2		2	Sc1	333.0
Sc2:	2	Ni	274.3	Sc2:	2	Rh	276.9
	2	Ni	276.7		2	Rh	278.5
	2	In2	306.2		2	In2	312.4
	2	In1	312.9		2	In1	317.8
	2	In2	319.2		2	In2	323.3
	2	Sc2	335.2		2	Sc2	333.0
	1	Sc3	346.6		1	Sc3	355.8
	1	Sc3	364.0		1	Sc3	370.7
	2	Sc2	390.9		2	Sc2	396.2
Sc3:	2	Ni	260.0	Sc3:	2	Rh	263.3
	2	In1	299.1		2	In1	302.8
	2	In2	306.2		2	In2	309.0
	2	In1	317.8		2	In1	319.9
	1	Sc1	319.9		1	Sc1	322.9
	2	Sc3	335.2		2	Sc3	333.0
	1	Sc3	348.0		1	Sc3	353.0
	1	Sc2	346.6		1	Sc2	355.8
	1	Sc2	364.0		1	Sc2	370.7
Ni:	2	Sc3	260.0	Rh:	2	Sc3	263.3
	2	Sc2	274.3		2	Sc2	276.9
	2	Sc2	276.7		2	Sc2	278.5
	1	In2	275.6		1	In2	285.5
	1	In1	283.4		1	In1	288.9
	1	In2	303.8		1	In2	310.9
In1:	1	Ni	283.4	In1:	1	Rh	288.9
	2	Sc3	299.1		2	Sc3	302.8
	2	Sc1	303.8		2	Sc1	305.3
	1	In2	314.5		1	In2	315.1
	2	Sc2	312.9		2	Sc2	317.8
	2	Sc3	317.8		2	Sc3	319.9
	2	In1	335.2		2	In1	333.0
	1	In1	383.9		1	In1	390.7
In2:	1	Ni	275.6	In2:	1	Rh	285.5
	1	Ni	303.8		2	Sc3	309.0
	2	Sc2	306.2		1	Rh	310.9
	2	Sc3	306.2		2	Sc2	312.4
	1	In1	314.5		1	In1	315.1
	2	Sc1	314.6		2	Sc1	315.5
	2	Sc2	319.2		2	Sc2	323.3
	2	In2	335.2		2	In2	333.0

All distances within the first coordination spheres are listed. Standard deviations are all equal or less than 0.2 pm.

ACKNOWLEDGMENTS

We thank the Degussa-Hüls AG for a generous gift of rhodium powder, and H.-J. Göcke for the work at the scanning electron microscope. M. L. is indebted to the NRW Graduate School of Chemistry for a PhD stipend.

REFERENCES

[1] Andersson, S. Angew Chem 1983, 95, 67.
[2] Parthé, E.; Chabot, B. In Handbook on the Physics and Chemistry of Rare Earths Gschneidner, K. A., Jr.; Eyring L. (Eds.); North-Holland: Amsterdam, 1984; Vol. 6, p. 113.
[3] Cenzual, K.; Parthé, E. Acta Crystallogr, Sect C: Cryst Struct Commun 1984, 40, 1127.
[4] Parthé, E.; Chabot, B.; Cenzual, K. Chimia 1985, 39, 164.
[5] Parthé, E. Elements of Inorganic Structural Chemistry, Pöge: Leipzig, 1990.
[6] Parthé, E.; Gelato, L.; Chabot, B.; Penzo, M.; Cenzual, K.; Gladyshevskii, R. In Gmelin Handbook of Inorganic and Organometallic Chemistry, 8th ed; Springer-Verlag: Berlin, 1993.
[7] Kalychak, Ya. M.; Zaremba, V. I.; Pöttgen, R.; Lukachuk, M.; Hoffmann, R.-D. In Handbook on the Physics and Chemistry of Rare Earths; Gschneidner, K. A., Jr.; Pecharsky, V. K.; Bünzli, J.-C. (Eds.); Elsevier, Amsterdam 2005, 34, 218.
[8] Rieger, W.; Nowotny, H.; Benesovsky, F. Monatsh Chem 1964, 95, 1502.
[9] Lukachuk, M.; Pöttgen, R. Z Kristallogr 2003, 218, 767.
[10] Becher, H. J.; Krogmann, R.; Peisker, E. Z Anorg Allg Chem 1966, 344, 140.
[11] Zaremba, V. I.; Kalychak, Ya. M.; Zavalii, P. Yu.; Bruskov, V. A. Krystallografiya 1991, 36, 1415.
[12] Emsley, J. The Elements, 3rd ed; Oxford University Press, Oxford, 1999.
[13] Lukachuk, M.; Pöttgen, R. Z Naturforsch, B: Chem Sci 2002, 57, 1353.
[14] Lukachuk, M.; Hoffmann, R.-D.; Pöttgen, R. Monatsh Chem 2005, 136, 127.
[15] Lukachuk, M.; Zaremba, V. I.; Hoffmann, R.-D.; Pöttgen, R. Z Naturforsch, B: Chem Sci 2004, 59, 182.
[16] Compton, V. B. Acta Crystallogr 1958, 11, 446.
[17] Dwight, A. E.; Downey, J. W.; Connor, R. A., Jr. Acta Crystallogr 1961, 14, 75.
[18] Donohue, J. The Structures of the Elements; Wiley; New York, 1974.
[19] Pöttgen, R.; Gulden, Th.; Simon, A. GIT-Laborfachzeitschrift 1999, 43, 133.
[20] Yvon, K.; Jeitschko, W.; Parthé, E. J Appl Crystallogr 1977, 10, 73.
[21] Sheldrick, G. M. SHELXL-97: Program for Crystal Structure Refinement; University of Göttingen: Göttingen, Germany, 1997.